

Available online at [www.sciencedirect.com](http://www.sciencedirect.com)

ScienceDirect

journal homepage: [www.keaipublishing.com/foar](http://www.keaipublishing.com/foar)SOUTHEAST  
UNIVERSITY

## RESEARCH ARTICLE

# Study of wind towers with different funnels attached to increase natural ventilation in an underground building

C.A. Varela-Boydo <sup>a,\*</sup>, S.L. Moya <sup>a</sup>, R. Watkins <sup>b</sup><sup>a</sup> *Tecnológico Nacional de México, Centro Nacional de Investigación y Desarrollo Tecnológico, Interior Internado Palmira s/n, Colonia Palmira, Cuernavaca, 62490 Morelos, Mexico*<sup>b</sup> *Kent School of Architecture & Planning, University of Kent, UK*

Received 8 January 2020; received in revised form 19 May 2020; accepted 24 May 2020

**KEYWORDS**Wind towers;  
Passive cooling;  
Natural ventilation;  
Funnels;  
CFD;  
Wind catchers

**Abstract** Finding ways to cool buildings by natural, passive techniques is crucial in the context of global warming. For centuries, wind towers (traditional windcatchers) have been used in the Middle East for cooling purposes. In this study, the use of funnels at the openings of wind towers for wind ingress and egress is proposed primarily to increase the mass flow captured by the wind tower. The use of funnels in the wind ingress openings increases the inlet area, improving the capture of wind. In parallel, the use of funnels in the egress openings modifies the wake of the tower, which aims to ease the exit of the flow from inside the building. Several design configurations are presented, where the length and width of the funnels are changed and tested separately by computational fluid dynamics (CFD). Results of over 120 CFD simulations are presented and compared. The volumetric flow entering the wind towers increases by 10.7% in several cases. These results indicate that adding funnels to wind towers could positively influence their performance. Changing the dimensions of the funnels affects their efficacy and can increase or decrease the airflow entering the tower.

© 2020 Higher Education Press Limited Company. Publishing Services by Elsevier B.V. on behalf of KeAi. This is an open access article under the CC BY-NC-ND license (<http://creativecommons.org/licenses/by-nc-nd/4.0/>).

\* Corresponding author.

E-mail address: [c.a.varela.boydo@gmail.com](mailto:c.a.varela.boydo@gmail.com) (C.A. Varela-Boydo).

Peer review under responsibility of Southeast University.

<https://doi.org/10.1016/j.foar.2020.05.007>

2095-2635/© 2020 Higher Education Press Limited Company. Publishing Services by Elsevier B.V. on behalf of KeAi. This is an open access article under the CC BY-NC-ND license (<http://creativecommons.org/licenses/by-nc-nd/4.0/>).

Please cite this article as: Varela-Boydo, C.A et al., Study of wind towers with different funnels attached to increase natural ventilation in an underground building, *Frontiers of Architectural Research*, <https://doi.org/10.1016/j.foar.2020.05.007>

## 1. Introduction

Buildings consume 30% of global electricity production, and this amount is expected to increase to 70% by 2050 (Jomehzadeh et al., 2017). Furthermore, they are responsible for approximately 40% of greenhouse gas emissions (Jomehzadeh et al., 2017). Overall, heating, ventilation, and air conditioning systems represent more than 60% of all energy consumed in buildings (Jomehzadeh et al., 2017). However, the amount and type of energy consumed can differ depending on climatic conditions. For example, the electricity consumed by air conditioning systems in hot and humid regions is higher, particularly during summer, leading to greater economic and environmental consequences. In the residential sector, from 2% to 7% of a geographic region's total energy consumption is dedicated for cooling (Santamouris, 2016). Globally, around 4% of the total energy used for heating and cooling buildings is used for cooling. This percentage is expected to reach 35% in 2050 and even 61% in 2100 (Santamouris, 2016) primarily due to global warming effects, increased economic activities, and global population growth. Nevertheless, this consumption could decrease substantially if buildings are designed considering their geographical location, climatic conditions, wind speeds, predominant wind directions, and suitable materials in terms of their thermal properties, and by incorporating passive systems for natural ventilation (Santamouris and Kolokotsa, 2013; Manzano-Aguilario et al., 2015).

Traditional architectures of several Middle Eastern cultures offer examples of very ingenious solutions for cooling buildings by natural ventilation, such as the passive system for natural ventilation called Wind Towers. These systems are vertical rectangular structures with one or several channels in their interior and integrated with the buildings. In their upper part, apertures are oriented in the direction of the prevailing winds to facilitate their capture. Once the wind is captured, it flows through smaller cross-section channels, increases its speed, and is then channeled through the building, providing comfort to occupants without need of electromechanical air conditioners.

A considerable amount of work has been published on the operation and capacity of wind towers to increase natural ventilation in buildings. Moreover, the interest in their integration into modern buildings has increased and has been documented. This work covers a) monitoring buildings with wind towers (Bahadori et al., 2008; Kalantar, 2009; Bouchahm et al., 2011), b) experiments with scale models in a wind tunnel supplemented with computational fluid dynamics (CFD) (Montazeri et al., 2010; Dehghan et al., 2013; Reyes et al., 2015; Afshin et al., 2016; Mohamadabadi et al., 2018), and c) studies only with CFD at full scale (Asfour and Gadi, 2006; Saffari and Hosseinnia, 2009; Reyes et al., 2013; Ghadiri et al., 2013; Hosseinnia et al., 2013; Hosseini et al., 2016; Benkari et al., 2017; Montazeri and Montazeri, 2018). Several of these studies refer purely to aerodynamic investigations, whereas others include heat transfer, effect of natural convection on walls, and "chimney effect" of towers; a few studies have considered the extra energy from the heat provided by the occupants. The incorporation of humidifying media at the beginning or end of the collection channels of the towers

has been reported to be very effective in increasing the air cooling in dry regions.

In aerodynamic studies, the effect of the speed and angle of incidence of the wind on the performance of towers has been considered as well as many other parameters, including the number and size of the inlet and outlet openings, and the location of the egress openings in the buildings. The effect of the dimensions of the tower as well as the distribution of the channels and the shape of the catchers and roofs of the buildings have been studied. The traditional concept of a wind tower has evolved into what is known as a commercial wind tower or windcatcher (Hughes et al., 2012; Calautit and Hughes, 2014; Ameer et al., 2016; Hughes and Mak, 2011) mounted on roofs of modern buildings, and it has proven very useful in improving natural ventilation in all cases. It has also evolved into different forms (Haw et al., 2012) with cylindrical geometries on rolling discs to catch winds in all directions (Dehghani-Sanij et al., 2015; Montazeri, 2011). In addition, traditional and modern forms have been integrated with other types of technologies, such as solar and geothermal energy (Benhammou et al., 2015), and horizontal and vertical heat transfer devices (Calautit et al., 2013; Calautit, O'Connor and Hughes, 2016; Calautit et al., 2017), which could extend the use of wind towers to winter conditions. Various reviews describing these technologies have been published (Jomehzadeh et al., 2017; Haw et al., 2012; Dehghani-Sanij et al., 2015; van Hooff et al., 2017).

In this work, the use of funnels is proposed to boost the airflow that enters buildings through wind towers. Very limited information can be found in the literature regarding the modification of existing wind towers to improve their aerodynamics and consequently, the natural ventilation of the buildings that have them. Thus, the present work focuses on improving the traditional wind tower design in terms of aerodynamics and aims to enhance natural ventilation technologies.

The use of funnels in ingress openings increases the opening area to catch the wind. In parallel, the use of funnels is also proposed for egress openings to modify the aerodynamic structures in the wake of the tower and facilitate or ease the exit of the air flowing from inside the building. The present study focuses only on increasing the volumetric airflow in wind towers. Several variables can affect the performance of wind towers, such as air temperature, air density, wind velocity, and wind direction in particular, among others that have been documented (Montazeri et al., 2010) (Dehghan et al., 2013; Afshin et al., 2016; Mohamadabadi et al., 2018). However, the main variable with the greatest effect on volumetric flow of air naturally ventilating the buildings is wind velocity in all cases. Therefore, this investigation proposes changing the strategy by using a single variable to test several designs and study only aerodynamics. Unlike the majority of previous studies, this work focuses on computing the differences only in the volumetric flow entering the towers. Wind tunnel testing of the traditional wind tower is presented. This study is followed by numerous CFD simulations that match the same experimental conditions but with various different funnels attached. Testing new funnels at various free stream velocities helps search for designs with a better performance than traditional wind towers in a simplified

manner. This study leads the way for future studies to test the best funnel designs in different operating conditions and consider more variables. This study aims to innovate and contribute toward a more sustainable society through developing alternative ventilation technologies.

## 2. Proposed geometrical model

A 1:25 tower model is introduced to evaluate the aerodynamic performance of the wind tower with the proposed enhancement geometries. Its shape is based on traditional designs of the Middle East, while it is connected to an underground building with dimensions similar to those of a small house. Fig. 1 shows the dimensions of the actual prototype used in wind tunnel testing, which was manufactured with 3 mm-thick acrylic sheets.

For the curved model parts, CAD files were created and then converted to G-Code to be manufactured using a 3D printer. The printer was configured to deposit 0.01 mm layers of PLA plastic. The finished parts were partially sanded and covered with transparent tape to ensure that the walls in contact with the fluid were completely smooth. A photograph of the experimental model is shown in Fig. 2. The model had a very large channel inside the room. This channel was installed to create an alignment zone for the flow entering the room and to have more accurate airflow measurements. Furthermore, four stands were installed to help the model stay in place during the testing and ensure that the tower was at the right height (H) inside the wind tunnel at all times. This step was necessary because several limitations of the wind tunnel prevented the model from being installed at the bottom and required it to be mounted upside down.

## 3. Wind tunnel testing

The main objective of this work is to present alternatives for increasing the airflow ingress to the wind tower by improving its aerodynamics. We decided to test only the tower inside the wind tunnel but connected it to a

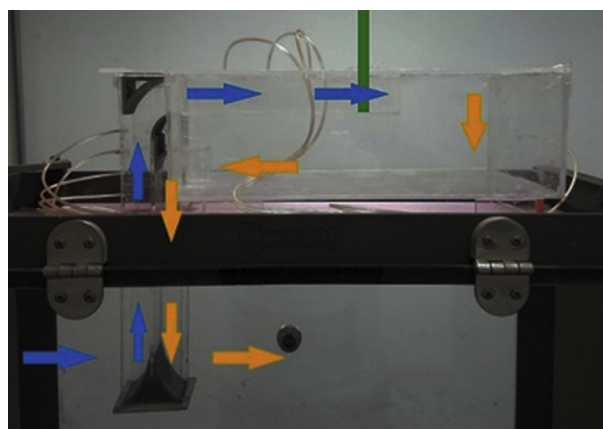


Fig. 2 Model in the wind tunnel: the arrows show the wind direction, where blue represents air entering the building, yellow represents air exiting the building, and green marks the flow sensor.

representation of an underground building outside the test section. The underground building was attached because it had a considerable aerodynamic load that the tower had to overcome.

Many of the previously cited papers reported different variables that affect the flow, such as wind direction (Mohamadabadi et al., 2018; Asfour and Gadi, 2006), tower surroundings, including the main building (Benkari et al., 2017), and roof topography (Ameer et al., 2016). Wind velocity was the variable that affected airflow the most in all cases. For the experimental phase of the present work, we decided to compute only the volumetric flow captured by the tower (and flowing to the inside of the building) as the free stream velocity increased in a single direction. Measurements were made using an open-circuit Eiffel-type wind tunnel housed inside a hermetically sealed room (Fig. 2). Its test section had dimensions of 0.35 m × 0.35 m × 0.6 m. The scale model wind tower's cross-section was under one-eighth of the wind tunnel cross-sectional area, allowing the air to flow freely around

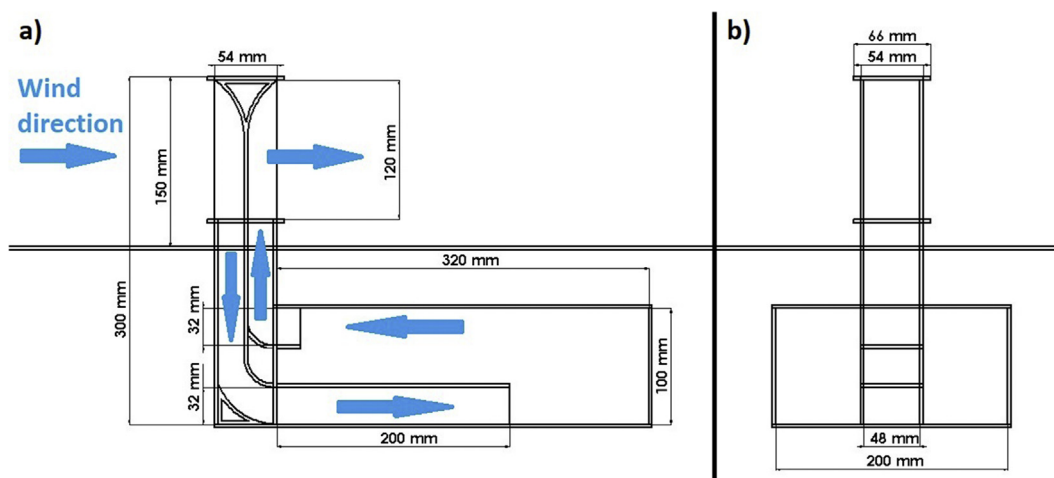


Fig. 1 Experimental model dimensions: a) side view of the model with arrows showing the path that the air follows, b) front view of the model in line with the wind direction.

it. In several published works of building aerodynamics, the aspect ratio of the wind tower and the test section were larger. During preliminary tests, we found that under the present configuration, the aspect ratio was sufficient to represent the phenomenon, while the tower caught sufficient air to activate the sensors at their optimal operational window. The tower was not a typical building mainly because a portion of the flow that interacted with it actually entered the building and then exited right in the wake, modifying the same. This interaction allowed the use of smaller domains, a practice that is also present in the literature; several of the published manuscripts that used similar proportions are (Afshin et al., 2016; Reyes et al., 2013; Benkari et al., 2017; Ameer et al., 2016; Hughes and Mak, 2011; Haw et al., 2012; Calautit et al., 2013; Elmualim, 2006; Sadeghi and Kalantar, 2018; Heidari et al., 2017). The model was positioned upside down 150 mm behind (downstream) the test section's starting point. Inlet and egress openings were 48 mm × 120 mm. The entire H of the tower was 303 mm, but only 150 mm was inside the wind tunnel. The tower was connected to a scale room that was 100 mm in H, 200 mm in width, and 320 mm in length (L). The room had two ducts inside, one of 200 mm for the ingress flow and another of 20 mm for the egress.

The wind tunnel was equipped with an axial fan, which was powered by an electric motor controlled by a variable frequency drive and capable of modifying the power in increments of 0.01%. For the tests, the fan was set to move the air at speeds from 5 m/s to 17.5 m/s in increments of 2.5 m/s. Six different free stream velocities were used. Considering the H of the tower inside the wind tunnel as the L scale, the Reynolds number ranged from 51,344 to 179,704. In all cases, the temperature was the same and stable (21 °C). The turbulence intensity in the test section inlet remained under 1% during measurements. The volumetric flow in the wind tower ducts was recorded, and the data were used to calibrate the numerical model used in the CFD simulation phase. An electronic probe was installed inside the ingress duct 0.16 m away from the tower to measure the airflow inside the ducts. That distance was set to let the air flowing through the duct align sufficiently to achieve consistent measurements. A hot wire anemometer was used to measure the flow, as also reported by (Calautit and Hughes, 2014; Ameer et al., 2016; Hughes and Mak, 2011; Calautit, O'Connor, and Hughes, 2016; Calautit et al., 2017; Elmualim, 2006). This instrument (from Extech) had a resolution of 1.5e−3 m/s and an accuracy of ±3%. Following the procedures presented in previously mentioned references, the data presented were averages of values collected during 180 s of measurements for the six wind speeds selected. The flow inside the tunnel was allowed to settle between each measurement before data were collected. The uncertainty values of the experimental data for the first three wind speeds were 1.03%, 0.92%, and 0.84% respectively, whereas the last three had values of 0.66%, 0.61%, and 0.55% respectively. A graph of the values would show that the uncertainty of the data decreased as the wind speed increased. Furthermore, the first three wind speeds had a different slope compared with the last ones.

#### 4. Enhanced geometry models

Commercial CAD software was used to create the geometries that were exported to the ANSYS Workbench interface for further use. Various simplifications were made during the design phase: the tower inlet would always be for air ingress, and the outlet would only work as an exit for the fluid. At full scale, the tower would be installed in an area with one predominant wind direction. In further studies, towers capable of redirecting the inlet will be tested to always face the wind direction, as proposed by (Dehghani-Sanij et al., 2015). Another simplification was that no walls or windows were installed in the underground building, only an ingress duct and an egress duct both with an L of 20 mm. For the enhanced geometries, a duct shorter than that in the experimental model was modelled. Two geometric models of the building were used for the CFD simulation phase of this work: one replicating the experiment and another with a shorter ingress duct inside the room.

Nine different geometric configurations were selected for the inlet funnels. Fig. 3 shows that funnels with straight walls were added to the towers. The element's L was set to 24, 18, and 12 mm, while the H was set to 9, 6, and 3 mm. The same nine funnel dimensions were selected for the outlet funnels; in these last ones, they served as exit area reductions, while those for ingress served to increase the tower's inlet area. This decision was taken to have the same percentage difference between the original opening and the openings of the different funnels.

Ingress and egress funnels were tested separately. In further studies, they will be tested together because inlet funnels modify the wind structures in the wake, which modifies the egress funnel aerodynamics. However, as a confirmation, the best-performing ingress and egress funnels were added to the wind tower to compute one set of simulations and evaluate the combined performance.

Fig. 3 shows that the higher and lower elements of the ingress funnels and the egress funnels are parallel, unlike traditional funnels. Preliminary studies showed that the aerodynamic performance improves this way in both configurations. Changes in the opening area are presented in Fig. 4. The lateral elements open in different directions but with the same increments.

Even when the H of the opening remained the same in all cases, the width changed as the H increments. The opening areas were smaller than one-eighth of the test volume cross-section in all configurations. Figs. 5 and 6 show all ingress and egress funnels used during simulations, respectively.

The opening area for ingress and egress openings depended only on the H; therefore, both groups had only three different opening areas. Table 1 shows the dimensionless comparison between the openings of the different funnels and the opening of the original tower.

Each design will be named after its geometry for differentiation moving forward. The names of ingress funnels will start with IF, and those of egress funnels will start with EF. These letters will be followed by a dash and a nomenclature of the L and H of the funnel. For example, an ingress funnel with an L of 24 mm and an H of 3 mm will be referred to as IF-L24H03, and an egress funnel with an L of 12 mm and an H of 6 mm will be named EF-L12H06.



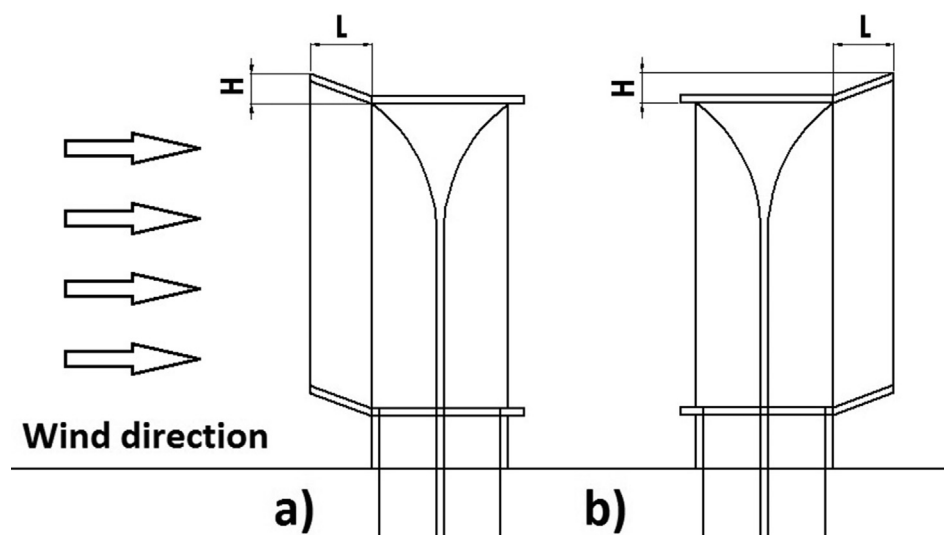


Fig. 3 Side profile of the towers: a) with ingress funnels, b) with egress funnels.

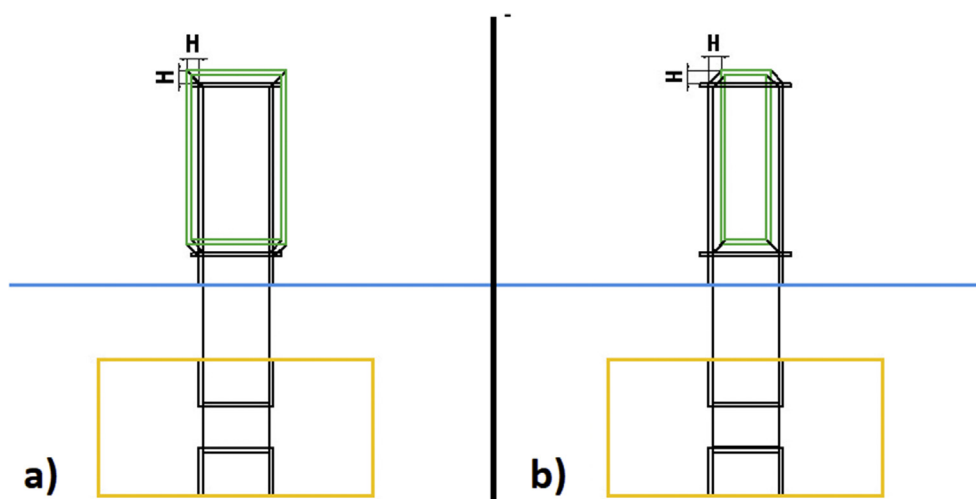


Fig. 4 View of the towers with enhanced geometries inside the test section: a) ingress funnels, b) egress funnels. In both cases, the representation of the wind tunnel test section is colored in blue, the room in orange, and the openings created by the funnels in green.

## 5. Meshing

Meshing is a very complex flow; thus, many meshing configurations were tested for different geometric models. After many considerations, a mesh comprised only of tetrahedrons was selected. Moreover, only one-half of the model was simulated, setting a symmetry boundary condition in the middle plane of the tunnel parallel to the flow. Several convergence tests were performed to determine a configuration with consistent results. The configuration was selected to avoid an excess of elements that could saturate the computer's memory and the motherboard bus while simulating cases simultaneously.

The initial mesh independence study was conducted with the original tower design and established a configuration for the mesh that does not interfere with the results.

However, several convergence problems were found when this configuration was used with the enhanced geometries. Complementary studies, such as changing the element size mainly in the funnels, were carried out simultaneously to ensure proper convergence and achieve results that are independent of the mesh. The results show that the element growth rate in the outer tower wall and the funnels must be reduced to avoid the formation of elements with angles smaller than  $30^\circ$ . As a starting point, a mesh was created, where all elements in contact with the walls had sizes to achieve a  $Y^+ = 1$  and growth ratios of 1.05. This mesh was extremely dense and had refinement in places where it was not needed. The next step was to increment the size of the element in non-critical areas, such as the wind tunnel walls, and the interior of the underground building. The value of  $Y^+$  for these areas was

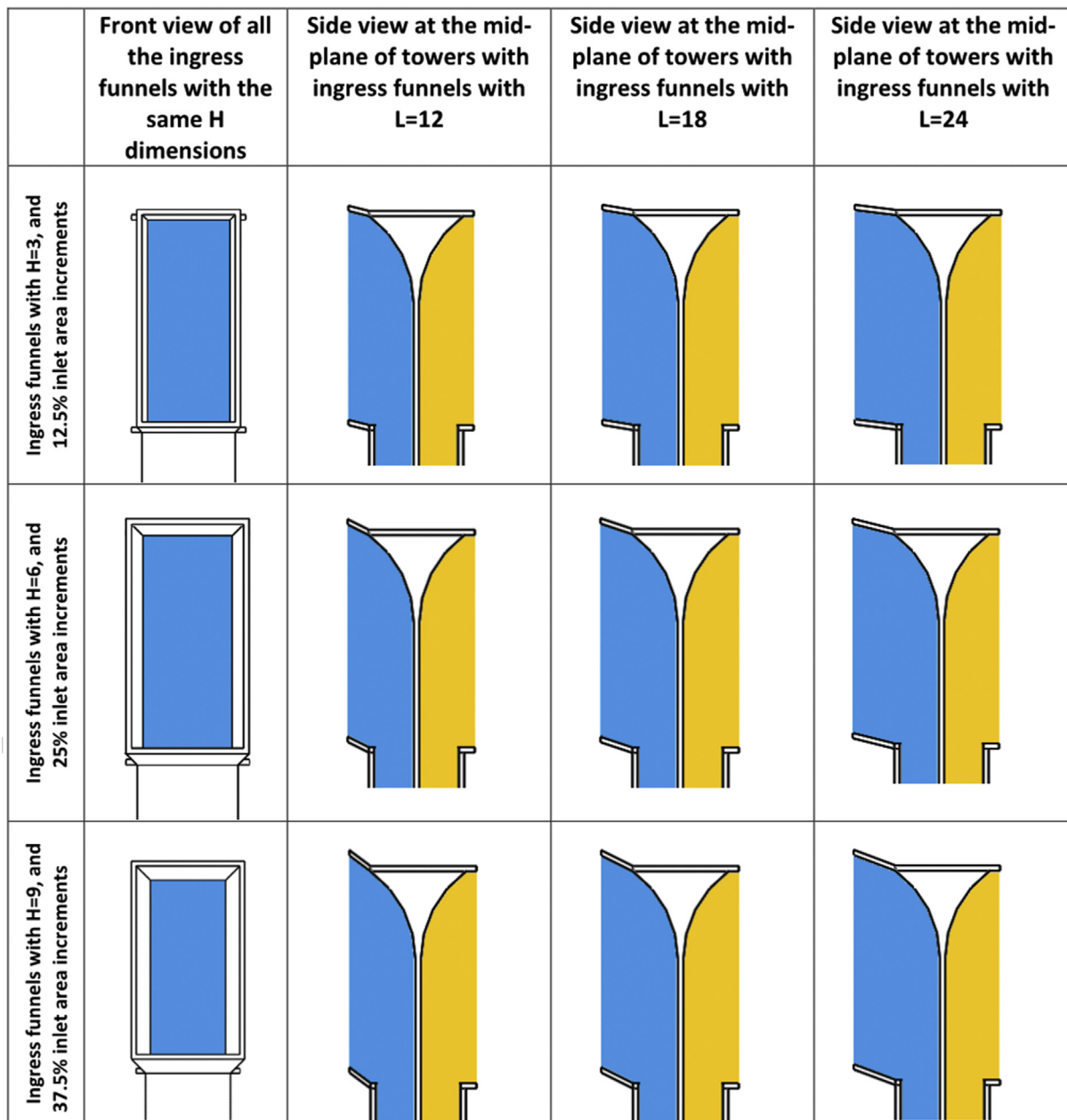


Fig. 5 Ingress funnels used during simulations. The inlets are displayed in blue, and the outlets are displayed in yellow.

incremented at different rates. The results of the simulations did not show substantial differences until the values of  $Y^+$  reached much higher values. In parallel, the growth ratio was also incremented. The final values ranged from 1.10 to 1.20 over the domain. In the tower walls, the size of the elements was incremented to a 1.25  $Y^+$  value. Sensitivity analysis showed that these parts could also work with  $Y^+$  values of 5, but the meshes had smaller cell sizes to follow regular practice.

Two surface monitors were used to measure the mass flow captured by the tower and flowing inside and into the building: one in the vertical ingress duct and another in the vertical egress duct. These monitors were also used to assess the convergence of the results in the building. The

flow moved downward in the monitor placed in the vertical ingress duct and upward in the other. Meshes with a difference over 0.001% between both computed flows were discarded. Various velocity profiles were also traced inside and outside the building to ensure that the flow field is independent of the mesh, and the difference between wind velocity values is under 0.5% of relative error. Fig. 7 shows the mesh used in the largest funnel tested, together with the named sections of the regions.

A special control volume was set to ensure proper element size control in the mesh for the tower's wake. This control volume allowed a very specific element size to be assigned in the zone where more convergence problems were caused by shedding of multiple vortices. This

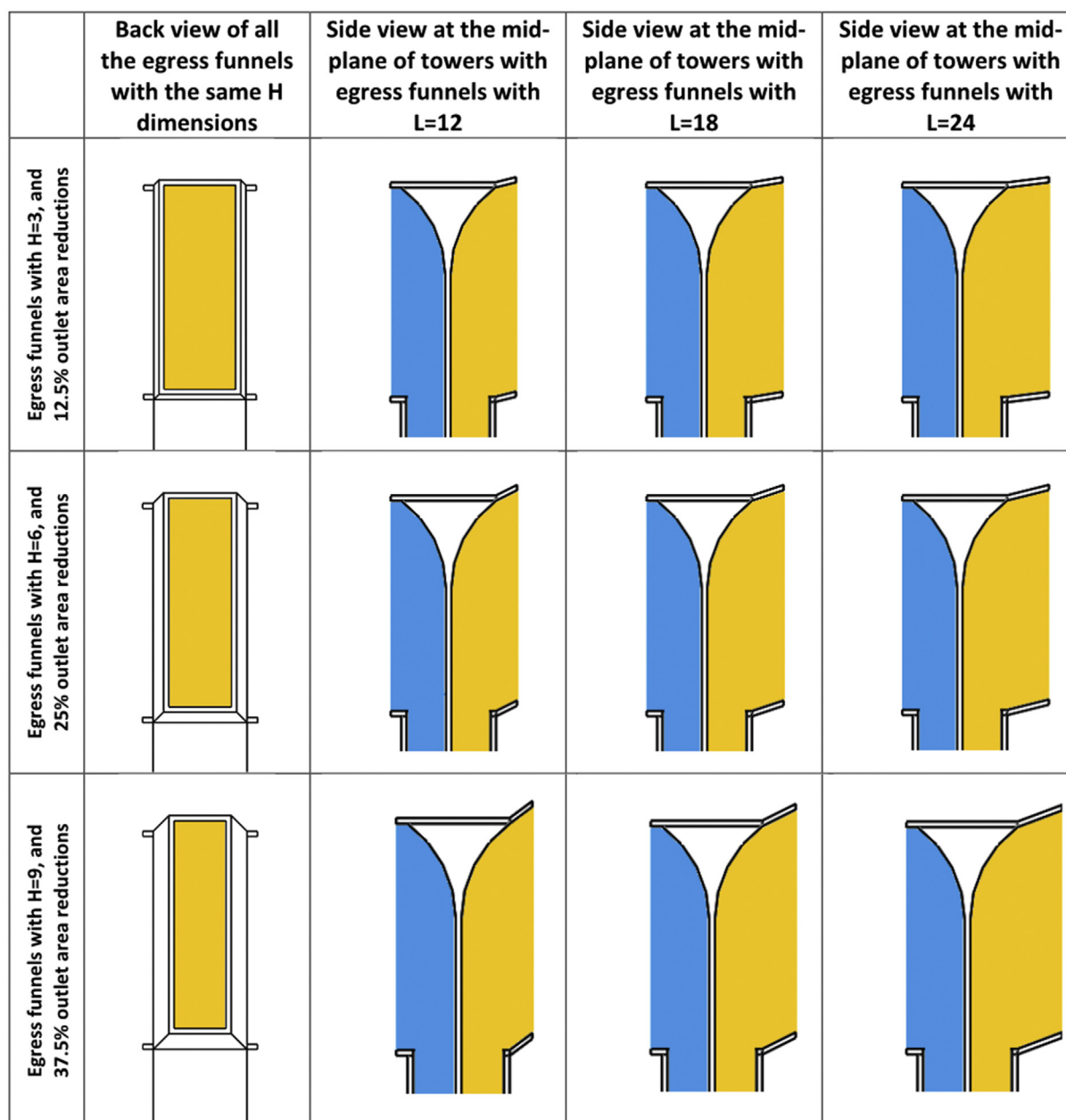


Fig. 6 Egress funnels used during simulations. The inlets are displayed in blue, and the outlets are displayed in yellow.

technique is very common in turbomachinery CFD simulations but has not been generally used in flows inside and around buildings. The domain dimensions follow those of the wind tunnel, with the exception of the width, which represents only one-half because of the use of a symmetry plane.

The number of elements increased with the increment in the size of the funnels and averaged 5.65 million elements, with a maximum size of 0.04 m. Table 2 shows the final element sizes for the different flow regions selected for 20 wind tower configurations.

In Fig. 7, the ingress duct inside the room is shorter than that in Figs. 1 and 2. As mentioned before, the air ingress duct to the room was shortened in the CAD model to save mesh elements. This wind tower, with the short ingress duct, was then modified by adding the funnels.

## 5.1. CFD simulation

For the numerical simulation phase of the work, ANSYS Fluent was selected as the tool to simulate the flow fields; this tool has been used by many researchers such as (Mohamadabadi et al., 2018; Hosseinnia et al., 2013; Hosseini et al., 2016; van Hooff et al., 2017; Heidari et al., 2017; Perén et al., 2015). A consensus about the right turbulence model to use in simulating the flow field inside and around the wind towers could not be found mainly because of numerous configurations available and documented in the literature by (Montazeri and Montazeri, 2018) and (van Hooff et al., 2017). In preliminary tests, the same models used in different publications were tested. Various configurations of the  $k-\epsilon$  turbulence model were used as in the

**Table 1** Dimensionless comparison between the original opening and the openings of the different funnels.

	Opening area of the funnels in comparison to the original opening
Ingress funnels with H = 3	1.125
Ingress funnels with H = 6	1.250
Ingress funnels with H = 9	1.375
Egress funnels with H = 3	0.875
Egress funnels with H = 6	0.750
Egress funnels with H = 9	0.625

work of (Hosseinnia et al., 2013), (Calautit, O'Connor, and Hughes, 2016), and (Heidari et al., 2017). Furthermore, different configurations of the  $k-\omega$  model were tested following the work of (Mohamadabadi et al., 2018), (Hosseini et al., 2016), and (Perén et al., 2015). The  $k-kl-\omega$  model was also used to widen the search, even when this model is not used often in this type of flow. The comparison of results between the different turbulence models and the wind tunnel testing is not presented in this manuscript. It will be published in a later paper showing in more detail the strong and weak points of each turbulence model when simulating this flow.

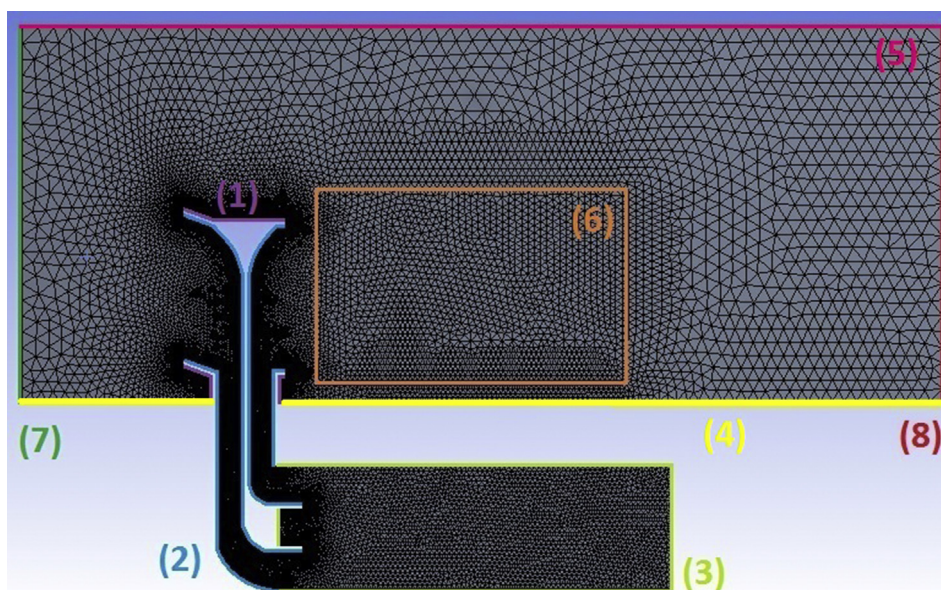
Overall, the  $k-\omega$  SST and the  $k-kl-\omega$  models achieved results closest to those obtained in the wind tunnel. In this case, the results of both models are similar. However, the  $k-kl-\omega$  needed more computer time, and no published papers could back up its selection; thus, it was discarded. The  $k-\omega$  SST model was selected for use during the entire numerical simulation phase of the work. In all cases, the equations in the ANSYS Fluent User's Guide (Release, 2017) were not modified and were used as found. These equations govern mass conservation, momentum conservation, energy conservation, turbulent kinetic energy, energy

**Table 2** Element sizes for the mesh.

	Region	Size (meters)
(1)	Outer tower wall	2.5e-5
(2)	Inner tower wall	2.1e-5
(3)	Room/house wall	4.0e-3
(4)	Wind tunnel wall 1	5.0e-3
(5)	Wind tunnel walls 2, 3	4.0e-2
(6)	Wake control volume	6.0e-3
(7)	Inlet	2.0e-2
(8)	Outlet	4.0e-2

dissipation rate, and specific rate of dissipation, among many other variables associated with different turbulence models.

For all funnel designs, six simulations were carried out at six different free stream inlet velocities from 5 m/s to 17.5 m/s in increments of 2.5 m/s. For the domain outlet, a pressure outlet was set at 0 Pa, and a second-order upwind scheme was adopted. For pressure-velocity coupling, the semi-implicit method for pressure-linked equation was used. A gravitational acceleration of  $+9.81 \text{ m/s}^2$  in the vertical (Y) direction was configured to replicate the experimental conditions. Regarding the convergence of each simulation, all standard values found in ANSYS Fluent User's Guide (Release, 2017) were used. Values for the convergence criterion were  $10^{-3}$  for all equations. In all cases, the iteration was completed when the set convergence criteria were met and the slope of the residuals' graphs was stable. Additionally and as mentioned before, if the difference computed between the monitors that measured the flow in the vertical ingress duct and the vertical egress duct was not close to zero, the particular simulation was not considered valid. In general, these conditions were met between 450 and 650 iterations

**Fig. 7** Symmetry plane for the simulation showing the mesh elements and highlighting the different zones configured.



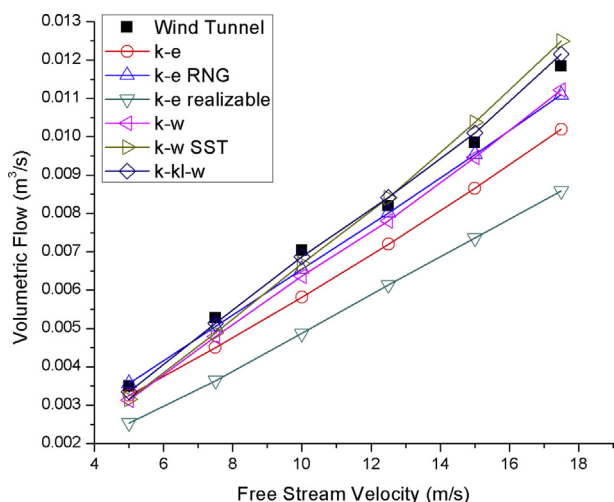


Fig. 8 Volumetric flow comparison between wind tunnel testing and CFD.

depending on the flow speed; those conditions with lower wind speeds converged after more iterations.

## 6. Results and discussion

### 6.1. Comparison between wind tunnel and CFD

After completing the wind tunnel testing, the original tower model was tested by CFD simulations with identical geometric dimensions and free stream velocity. Fig. 8 compares the volumetric flow measured in the wind tunnel and the flow computed in ANSYS Fluent by six turbulence models. The results shown are exclusive to the present manuscript and are not presented in the parallel paper mentioned earlier, that is, they come from what was learned from it.

The *k-kl-ω* and *k-ω SST* models performed better, followed by the *k-ε RNG* and standard *k-ω* models. The *k-ε*

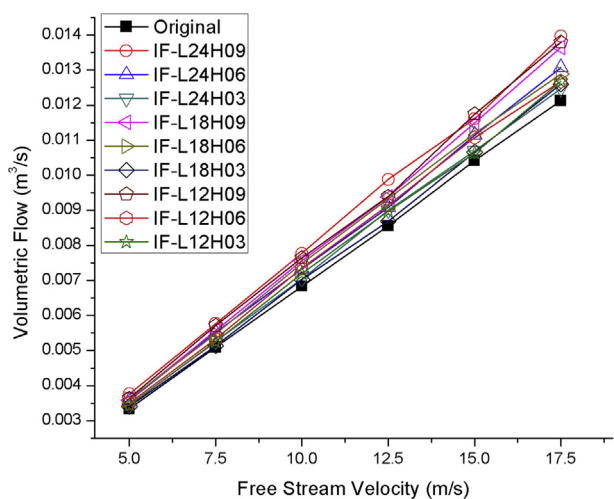


Fig. 9 Volumetric flow of the towers with ingress funnels at different free stream velocities.

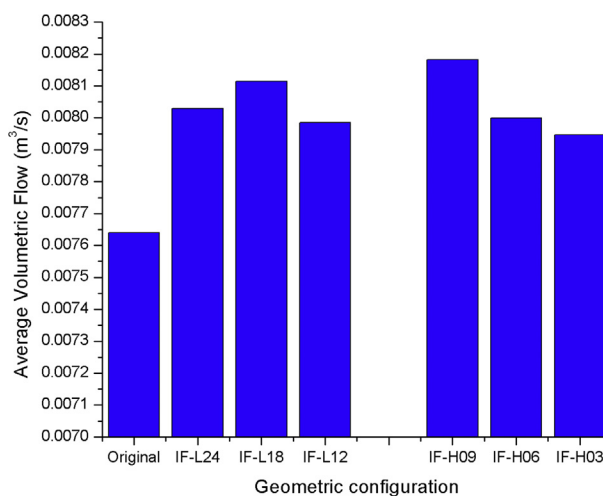


Fig. 10 Average volumetric flow for the different ingress funnel geometric configurations.

*standard* and *k-ε realizable* models had unsatisfactory results under the present conditions.

Considering the quality of the results and the computing time needed by each model, the *k-ω SST* model was selected to perform all simulations. On average, the relative error between this model and the wind tunnel testing was 5.31%, and the standard deviation was 5.36%. The CFD simulations under-predicted the volumetric flow in the duct for the first three free stream velocities but over-predicted it for the last three. In general, a similar behavior was found over the entirety of simulations and wind tunnel testing; the first three wind velocities showed one slope; then, in the same line graph, the slope changed for the last three whether funnels were installed. This finding suggests that changes in the flow structures modified the tower's air ingress and egress between 10 m/s and 15 m/s. This phenomenon may be explored in further research but is not considered here.

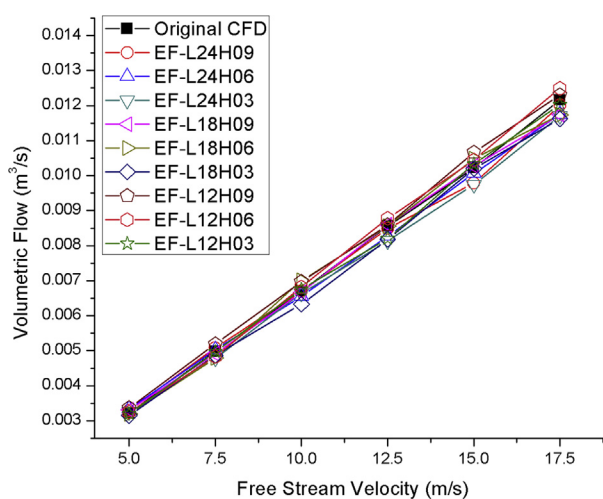
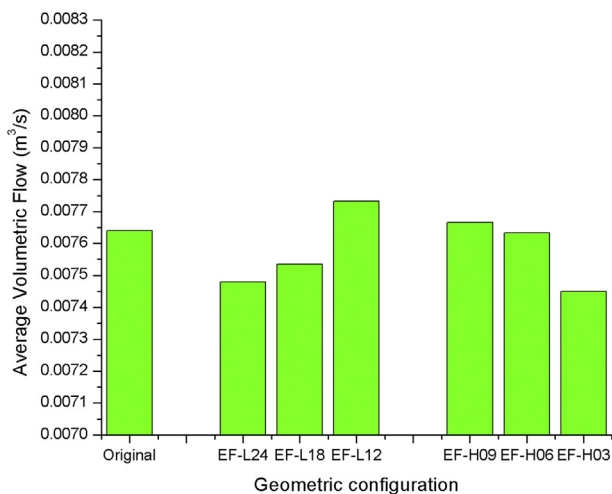


Fig. 11 Volumetric flow of the towers with egress funnels at different free stream velocities.



**Fig. 12** Average volumetric flow for the different ingress funnel geometric configurations.

## 6.2. Changes in mass flow caused by the implementation of funnels

Eighteen funnel geometric configurations were used: nine for ingress and nine for egress funnels. In addition, one geometric configuration using the best-performing ingress and egress funnels was tested, plus the original model with a shortened inlet duct. Twenty geometries were tested at six different free stream velocities, resulting in 120 converged simulations presented in this paper.

The results of adding ingress funnels to the wind towers are presented in Fig. 9. A volumetric flow increment was observed in the ducts in all cases. The ingress funnel with  $L = 18$  mm and  $H = 9$  mm (IF-L18H09) was capable of catching the most wind. It increased the flow by 7.58% on average over the six free stream velocities, followed closely by the IF-L24H09 with 7.20%. The IF-L12H03 funnel presented the least improvements, increasing the flow by only 2.18% on average.

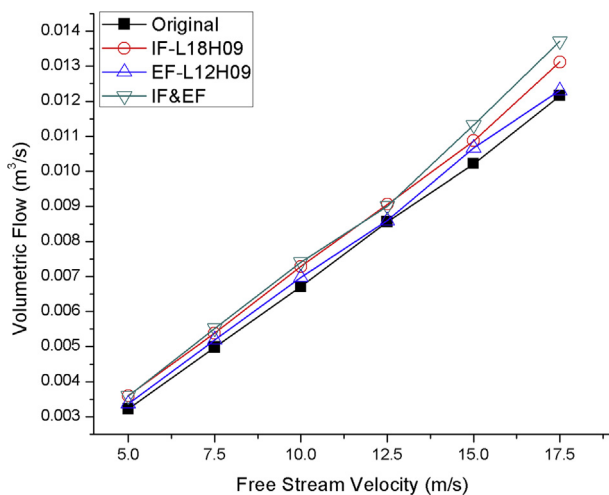


**Fig. 13** Volumetric flow of the towers with the best-performing funnels at different free stream velocities.

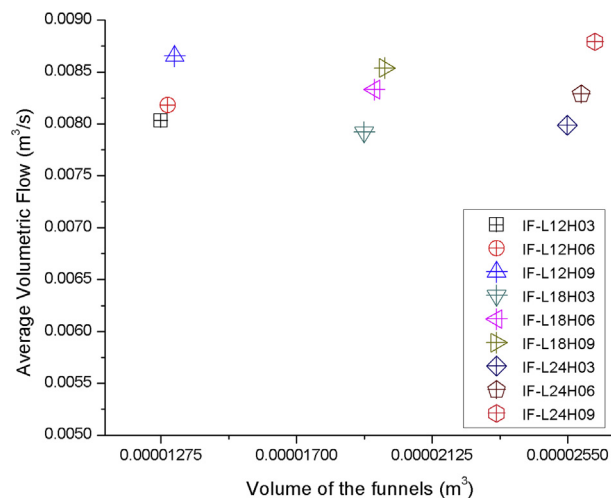


**Fig. 14** Average volumetric flow of the towers as a function of the volume of the ingress funnels.

Fig. 10 shows the same data, but it averages the flow of all the simulations with the same L and H and compares them with the original wind tower design. Ingress funnels with  $L = 18$  mm and  $H = 9$  mm had an average higher volumetric flow. Moreover, configurations with  $L = 12$  mm and  $H = 3$  mm had lower increments on average. Table 1 shows that ingress funnels with  $H = 9$  mm increased the opening area 37.5% but increased the average flow ingress by only 7.1%. Funnels with  $H = 6$  mm increased the opening area 25% but increased the average flow by 4.7%. Funnels with  $H = 3$  mm had openings 12.5% larger than the originals but increased the flow by 4.0% on average. These results show that in the present cases, the increment of the opening area is not followed by a proportional increment of the airflow. Changing the funnel L caused a different phenomenon. The increment of the L was used to create a longer funnel that could provide more space for the flow to get into the tower's duct more aligned. Data show that for the present cases, the increment of L did not guarantee

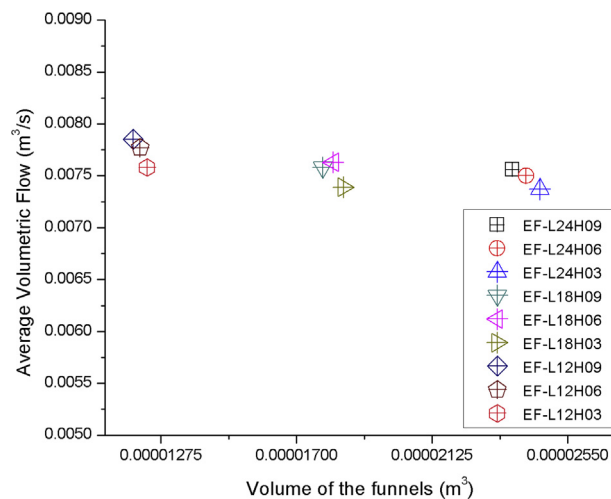


**Fig. 15** Average volumetric flow of the towers as a function of the volume of the egress funnels.

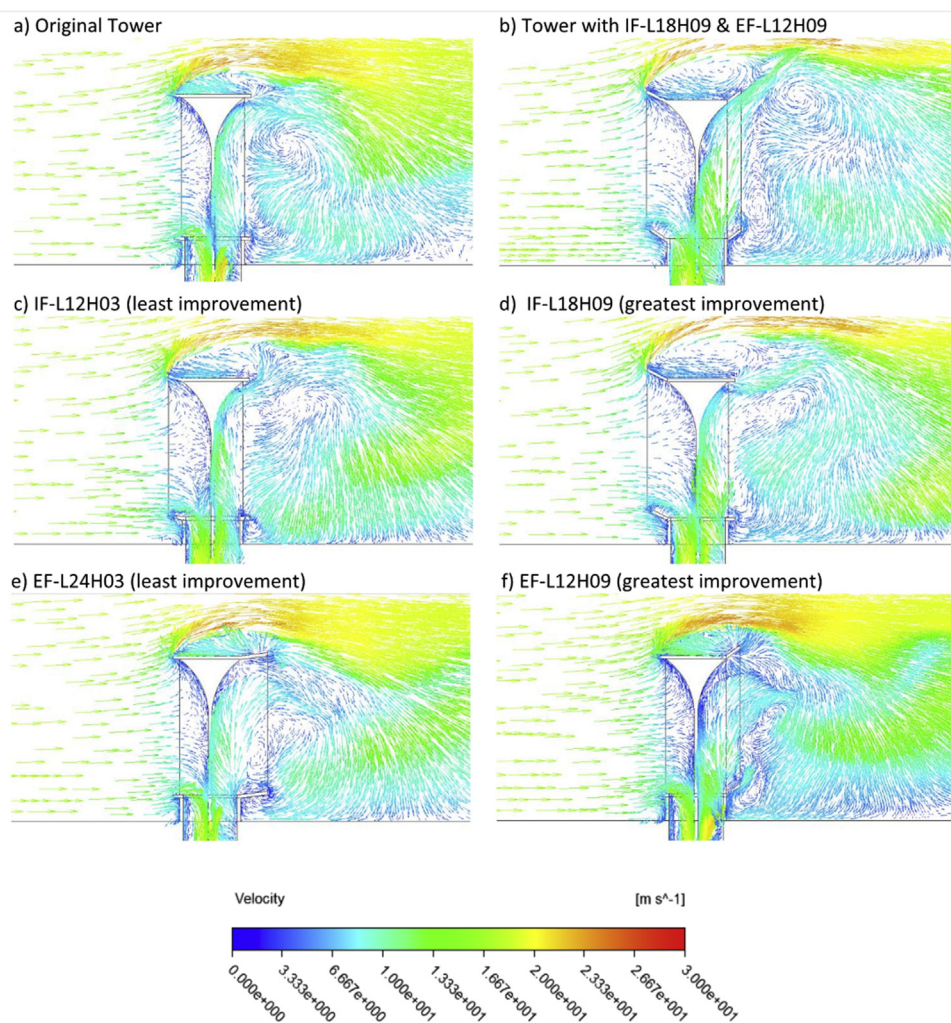


Fig. 16 Vector flow maps for different wind tower configurations at 17.5 m/s free stream velocity.

better performance, but it did have some consistency, showing that all ingress funnels with  $L = 18$  mm performed better than those with  $L = 24$  mm or  $L = 12$  mm.

For the egress funnels, the results are mixed, and many of the configurations decreased the airflow through the ducts, as shown in Fig. 11.

On average, the egress funnel with  $L = 12$  mm and  $H = 9$  mm (EF-L12H09) was capable of boosting the flow through the duct best, increasing the average airflow by 2.74% over the six free stream velocities. The EF-L24H03 performed the worst, reducing airflow by 3.44% on average. Seven of nine egress funnel designs reduced the flow in the ducts. The only egress funnels that improved performance were the EF-L12H09 and the EF-L12H06. Fig. 12 shows the same data as in Fig. 11, but it averages the airflow of all the simulations with the same  $L$  and  $H$  compared with the original wind tower design. On average, only egress funnels with  $L = 12$  mm and  $H = 9$  mm boosted the flow, whereas the rest reduced the performance. Egress funnels with  $L = 24$  mm and  $H = 3$  mm performed poorly.

Even when the results show that the majority of these configurations reduce the airflow, they prove useful to

understand that reducing the outlet area can boost performance in several of these cases. For example, egress funnels with  $H = 3$  mm and  $H = 6$  mm reduced the opening areas by 12.5% and 25%, respectively. Nevertheless, they had a lower flow than the egress funnel with  $H = 9$  mm, which had 37.5% smaller outlets than the original tower design. Summarizing the effects of changing the  $L$  of egress funnels on the flow, performance improves as egress funnels become shorter in the present cases.

Geometric models for inlet funnel IF-L18H09 and egress funnel EF-L12H09 were added to the original wind tower. One set of simulations at free stream velocities same as before was performed to test how they performed together.

Fig. 13 shows improvement in results. Independently, the IF-L18H09 increased airflow compared with the original wind tower's 7.58%, while the EF-L12H09 boosted it by 2.74%. When used together, they increased the flow by 10.7%, which is slightly more than the arithmetic sum and possibly caused by the alteration of the wake by the presence of the ingress funnel.



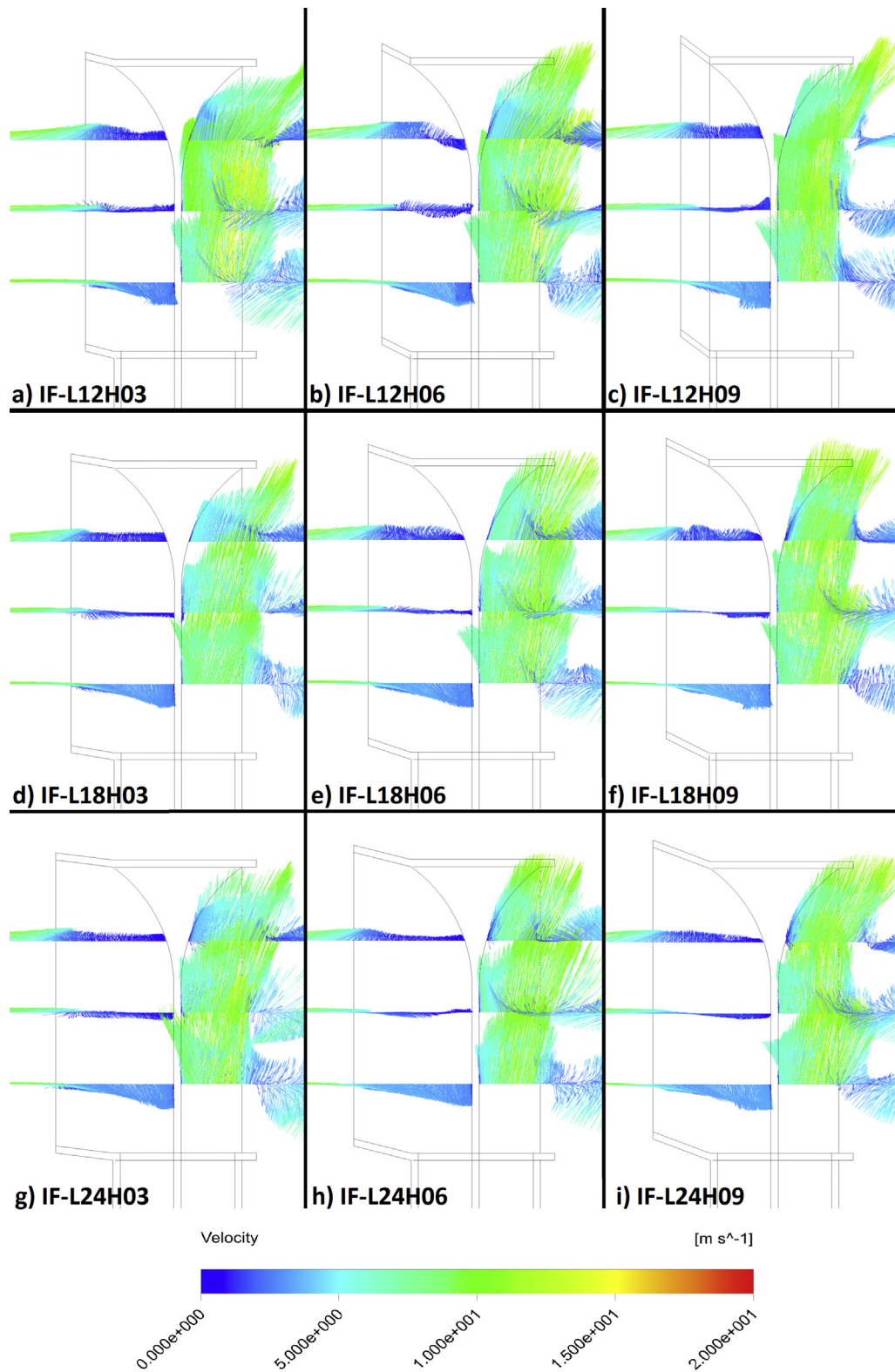


**Fig. 17** Side view of vector flow maps for different wind tower configurations at 12.5 m/s of free stream velocity and different heights.



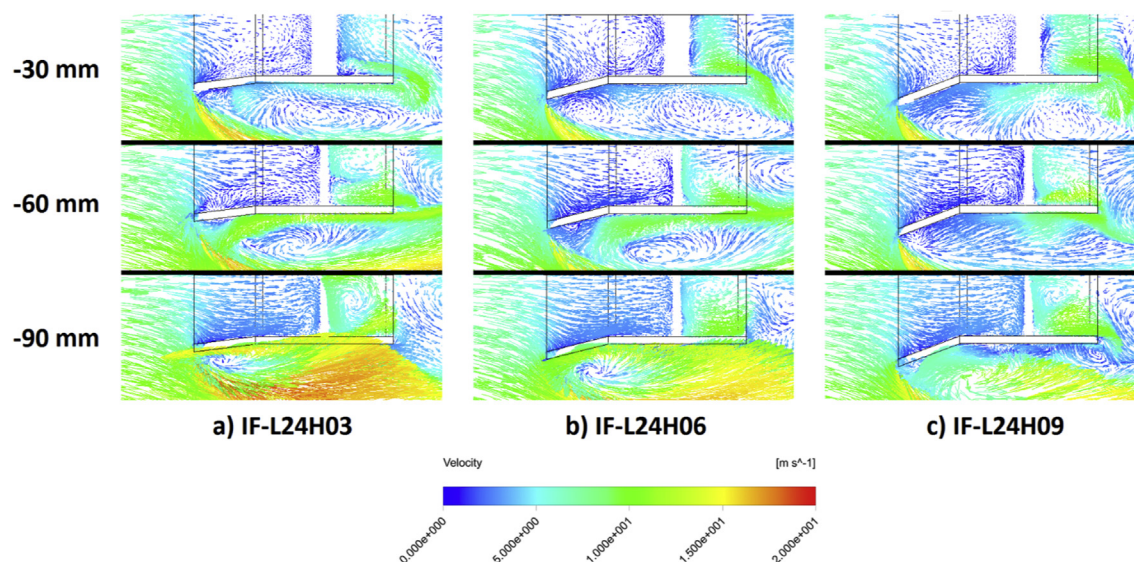


Fig. 18 Vector flow maps for wind towers with IF of  $L = 24$  at 12.5 m/s of free stream velocity and different heights.

### 6.3. Effects in mass flow caused by changing the volume of funnels

Figs. 14 and 15 show the average volumetric flow of the different models as a function of the volume of the funnels, enabling studying the effects of changing  $H$  and  $L$  simultaneously on the performance of the towers. Both figures show that the main variable that affects volume is  $L$ . The volume of the funnels changed more considerably with  $L$  increments, whereas the  $H$  increment represented a smaller change in volume. Regarding the effect of volume on the flow, two different behaviors are observed in the graphs. Fig. 14 shows that the change in volume of the funnel did not show great differences for the IF. In general, the average volumetric flow increased as the  $H$  increased, and volume did not seem to have an important effect on the flow. This finding is engaging because  $L$ , which is the variable with a greater effect on volume apparently had a less important effect over flow. Analysis of Fig. 15 reveals a tendency for the average flow to decrease with the volume of the funnel, that is, funnels with smaller volumes perform better.

### 6.4. Changes in the flow field

#### 6.4.1. Best- and worst-performing funnels

Fig. 16 illustrates the behavior of the flow around the original tower and the modified towers, and the velocity vector maps of the symmetry plane of simulations of six different cases at 17.5 m/s. The best- and worst-performing ingress funnels and egress as well as the result of combining the best funnels are presented. Together, they are compared with the original tower at the same free stream velocity.

In general, all six designs had the same problem: almost half of the flow in contact with the inlet opening did not enter the tower. Inside the inlet opening of the tower, half of the vectors went down and into the duct, while the other half went up and created an exit stream that left the tower.

This behavior prevented the building from receiving all the wind in contact with the tower. Ways to channel all the wind in contact with the tower must be found to increase the airflow in the buildings. Comparing the ingress funnels enabled appreciating differences in the vectors at the inlet openings. The IF-L18H09 design channeled the air more smoothly compared with the original and the IF-L12H03. The vortex present in the middle of the opening of the original tower and with IF-L12H03 decreased in size substantially in IF-L18H09, and this reason could explain the airflow boost. In parallel, the IF-L12H03 had much larger vortices in the inlet than the original design. However, it had a 12.5% larger opening than the original; therefore, it managed to catch more wind. Something different can be seen regarding the egress funnels: a very complex flow was present in all cases. What stands out the most is that many vectors in the outlet openings were in the opposite direction to the main flow, which means that the air was forced to the interior of the outlet. In the EF-L12H09 configuration, a minimal number of vectors entered the tower, which could explain the airflow increment. Finally, considering the design that combines both funnels, a completely new flow structure in the wake can be seen. The front showed a behavior similar to that of IF-L18H09. However, in the back, the vortices' position changed completely mainly because of the presence of the ingress funnel. Nevertheless, the presence of vectors entering the tower in the egress duct could be seen but in lower numbers than in the original tower.

#### 6.4.2. Behavior of the ascending currents in the flow

Figs. 17 and 18 are presented to study more deeply the ascending flow that briefly entered the funnel and then left the tower without entering the vertical duct to be measured and used inside the building. Fig. 17 shows vector maps of the flow at three different  $H$ s, with a 12.5 m/s wind velocity, to illustrate which parts of the flow inside the funnels are ascending and which ones are descending. The maps were positioned 30, 60, and 90 mm under the top of

the inlet opening. In general, when looking at the flow inside the nine different inlet funnels, the vectors of the lower maps tended to descend, those near the top tended to ascend, and the ones in the middle had mixed behaviors. Beyond this brief description, the correlation between the shape of the funnel and the direction of the flow inside of the same cannot be spotted or described in more detail. Fig. 18 helps understand this unpredictable behavior. It shows a perpendicular view of the maps at the same wind speed (12.5 m/s) but only for funnels with  $L = 24$ . Fig. 18 shows the flow inside and around the wind tower. Fig. 17 only shows the vectors from inside the funnels. Fig. 18 shows that the number of vectors going inside the tower increased as the H of the funnel increased in the maps placed 90 mm under the top of the inlets. A small vortex in the lower right corner of the inlet increased in size as the funnel grew in size. A similar behavior was found when comparing the maps placed 60 mm under the top of the opening. However, the size of the small vortex mentioned before increased in size considerably, and the number of vectors entering the towers was lower. As H increased, the total number of vectors increased, while the size of the vortex also grew.

Finally, the flow changed substantially for the map closest to the top. The majority of the space was occupied by the vortex, and even when several vectors entered the funnel, many evacuated from it. Using larger funnels apparently assisted in increasing the airflow entering the wind tower but also helped form vortexes inside the inlet opening that grow with funnel dimensions.

All these vector maps show that improving the aerodynamics of the towers is very important. A much higher airflow will be achieved by reducing the formation of vortexes in the inlets, channeling the entirety of wind in the same to the ducts, and reducing the air that flows back into the outlet. If the use of funnels is combined with new solutions that solve these problems, much more efficient natural ventilation systems would be achieved.

## 7. Conclusions

After analyzing 120 different simulations and wind tunnel tests, we conclude that increasing the opening area of the present wind towers by using funnels increases the volumetric flow entering the tower's ducts, although not proportionally. In the best case, increasing the H of the funnels to 9 mm improved performance by 7.1% on average, although the inlet opening is 37.5% larger than the original. Moreover, the L of the inlet funnels has a nonlinear effect on performance, and the models with an L of 18 mm performed better than shorter or longer ones.

Reducing the tower outlet area with funnels can modify the wind structures in the wake, which is sufficient to increase the airflow in the ducts. In this study, as the egress funnels become shorter in dimensions, the greater the flow they evacuate. Funnels with  $L = 12$  perform best. The opposite behavior is found regarding H, that is, performance improves as the H of the funnels increases.

New ways to capture the wind in contact with the ingress openings must be found because a large proportion of the flow creates a stream that leaves the tower before entering

the building. Additionally, new solutions to avoid the return of the air to the outlet must be developed. The results presented in this paper provide a foundation and pointers to advance research and develop funnel designs that may realize the full potential of wind towers for natural ventilation applications.

## Conflict of interest

There is no conflict of interest.

## Acknowledgement

The first author gives thanks to the CONACYT for their financial support.

## References

- Afshin, M., Sohankar, A., Manshadi, M.D., Esfeh, M.K., 2016. An Experimental Study on the Evaluation of Natural Ventilation Performance of a Two-Sided Wind-Catcher for Various Wind angles. *Renew. Energy* 85, 1068–1078.
- Ameer, S.A., Chaudhry, H.N., Agha, A., 2016. Influence of Roof Topology on the Air Distribution and Ventilation Effectiveness of Wind towers. *Energy Build.* 130, 733–746.
- Asfour, O.S., Gadi, M.B., 2006. Effect of integrating wind catchers with curved roofs on natural ventilation performance in buildings. *Architect. Eng. Des. Manag.* 2 (4), 289–304. Taylor & Francis.
- Bahadori, M.N., Mazidi, M., Dehghani, A.R., 2008. Experimental investigation of new designs of wind towers. *Renew. Energy* 33 (10), 2273–2281.
- Benhammou, M., Draoui, B., Zerrouki, M., Marif, Y., 2015. Performance Analysis of an Earth-To-Air Heat Exchanger Assisted by a Wind Tower for Passive Cooling of Buildings in Arid and Hot Climate. *Energy Convers. Manag.* 91, 1–11.
- Benkari, N., Fazil, I., Husain, A., 2017. Design and performance comparison of two patterns of wind-catcher for a semi-enclosed courtyard. *Int. J. Mech. Eng. Robots. Res.* 6 (5), 396–400.
- Bouchahm, Y., Bourbia, F., Belhamri, A., 2011. Performance Analysis and Improvement of the Use of Wind Tower in Hot Dry climate. *Renew. Energy* 36 (3), 898–906.
- Calautit, J.K., Hughes, B.R., 2014. Wind Tunnel and CFD Study of the Natural Ventilation Performance of a Commercial Multi-Directional Wind Tower. *Building And Environment* 80, 71–83.
- Calautit, J.K., Hughes, B.R., Chaudhry, H.N., Ghani, S.A., 2013. CFD analysis of a heat transfer device integrated wind tower system for hot and dry climate. *Appl. Energy* 112, 576–591.
- Calautit, J.K., Hughes, B.R., O'Connor, D., Shahzad, S.S., 2017. Numerical and Experimental Analysis of a Multi-Directional Wind Tower Integrated with Vertically-Arranged Heat Transfer Devices (VHTD). *Appl. Energy* 185, 1120–1135.
- Calautit, J.K., O'Connor, D., Hughes, B.R., 2016. A natural ventilation wind tower with heat pipe heat recovery for cold climates. *Renew. Energy* 87, 1088–1104.
- Dehghani-Sanjaj, A.R., Soltani, M., Raahemifar, K., 2015. A new design of wind tower for passive ventilation in buildings to reduce energy consumption in windy regions. *Renew. Sustain. Energy Rev.* 42, 182–195.
- Dehghan, A.A., Esfeh, M.K., Manshadi, M.D., 2013. Natural Ventilation Characteristics of One-Sided Wind Catchers: Experimental and Analytical evaluation. *Energy Build.* 61, 366–377.

- Elmualim, A.A., 2006. Effect of damper and heat source on wind catcher natural ventilation performance. *Energy Build.* 38 (8), 939–948.
- Ghadiri, M.H., Ibrahim, N.L.N., Mohamed, M.F., 2013. Performance evaluation of four-sided square wind catchers with different geometries by numerical method. *Eng. J.* 17 (4), 9–17.
- van Hooff, T., Blocken, B., Tominaga, Y., 2017. On the accuracy of CFD simulations of cross-ventilation flows for a generic isolated building: comparison of RANS, LES and experiments. *Build. Environ.* 114, 148–165.
- Haw, L.C., Saadatian, O., Sulaiman, M.Y., Mat, S., Sopian, K., 2012. Empirical study of a wind-induced natural ventilation tower under hot and humid climatic conditions. *Energy Build.* 52, 28–38.
- Heidari, A., Sahebzadeh, S., Dalvand, Z., 2017. Natural ventilation in vernacular architecture of Sistan, Iran; Classification and CFD study of compound rooms. *Sustainability* 9 (6).
- Hosseini, S.H., Shokry, E., Hosseini, A.A., Ahmadi, G., Calautit, J.K., 2016. Evaluation of airflow and thermal comfort in buildings ventilated with wind catchers: simulation of conditions in Yazd City, Iran. *Energy Sustain. Develop.* 35, 7–24.
- Hosseinnia, S.M., Saffari, H., Abdous, M.A., 2013. Effects of different internal designs of traditional wind towers on their thermal behavior. *Energy Build.* 62, 51–58.
- Hughes, B.R., Calautit, J.K., Ghani, S.A., 2012. The Development of Commercial Wind Towers for Natural Ventilation: A Review. *Appl. Energy* 92, 606–627.
- Hughes, B.R., Mak, C.M., 2011. A study of wind and buoyancy driven flows through commercial wind towers. *Energy Build.* 43 (7), 1784–1791.
- Jomehzadeh, F., Nejat, P., Calautit, J.K., Yusof, M.B.M., Zaki, S.A., Hughes, B.R., Yazid, M.N.A.W.M., 2017. A review on wind-catcher for passive cooling and natural ventilation in buildings, Part 1: indoor air quality and thermal comfort assessment. *Renew. Sustain. Energy Rev.* 70, 736–756.
- Kalantar, V., 2009. Numerical simulation of cooling performance of wind tower (Baud-Geer) in hot and arid region. *Renew. Energy* 34 (1), 246–254.
- Manzano-Agugliaro, F., Montoya, F.G., Sabio-Ortega, A., García-Cruz, A., 2015. Review of Bioclimatic Architecture Strategies for Achieving Thermal comfort. *Renew. Sustain. Energy Rev.* 49, 736–755.
- Mohamadabadi, H.D., Dehghan, A.A., Ghanbaran, A.H., Movahedi, A., Mohamadabadi, A.D., 2018. Numerical and experimental performance analysis of a four-sided wind tower adjoining parlor and courtyard at different wind incident angles. *Energy Build.* 172, 525–536.
- Montazeri, H., 2011. Experimental and numerical study on natural ventilation performance of various multi-opening wind catchers. *Build. Environ.* 46 (2), 370–378.
- Montazeri, H., Montazeri, F., 2018. CFD simulation of cross-ventilation in buildings using rooftop wind-catchers: impact of outlet openings. *Renew. Energy* 118, 502–520.
- Montazeri, H., Montazeri, F., Azizian, R., Mostafavi, S., 2010. Two-sided Wind Catcher Performance Evaluation Using Experimental, Numerical and Analytical modeling. *Renewable Energy* 35 (7), 1424–1435.
- Perén, J.I., Van Hooff, T., Leite, B.C.C., Blocken, B., et al., 2015. CFD analysis of cross-ventilation of a generic isolated building with asymmetric opening positions: impact of roof angle and opening location. *Build. Environ.* 85, 263–276.
- Release, 2017. *Ansys Fluent User's Guide*. Available at: <http://www.ansys.com>.
- Reyes, V.A., Moya, S.L., Morales, J.M., Sierra-Espinosa, F.Z., 2013. A study of air flow and heat transfer in building-wind tower passive cooling systems applied to arid and semi-arid regions of Mexico. *Energy Build.* 66, 211–221.
- Reyes, V.A., Sierra-Espinosa, F.Z., Moya, S.L., Carrillo, F., 2015. Flow field obtained by PIV technique for a scaled building-wind tower model in a wind tunnel. In: *Energy and Buildings*, 107, pp. 424–433.
- Sadeghi, H., Kalantar, V., 2018. Performance analysis of a wind tower in combination with an underground channel. *Sustain. Cities Soc* 37, 427–437.
- Saffari, H., Hosseinnia, S.M., 2009. Two-phase euler-Lagrange CFD simulation of evaporative cooling in a wind tower. *Energy Build.* 41 (9), 991–1000.
- Santamouris, M., 2016. Cooling the Buildings – Past, Present and Future. *Energy Build.* 128, 617–638.
- Santamouris, M., Kolokotsa, D., 2013. Passive Cooling Dissipation Techniques for Buildings and Other Structures: the State of the Art. *Energy Build* 57, 74–94.